Monthly Notices
of the
ROYAL ASTRONOMICAL SOCIETY

MNRAS **478,** 1595–1600 (2018)
Advance Access publication 2018 August 07

doi:10.1093/mnras/sty1188

A new strong-lensing galaxy at z= 0.066: another elliptical galaxy with a lightweight IMF

William P. Collier,★ Russell J. Smith and John R. Lucey
Centre for Extragalactic Astronomy, Department of Physics, University of Durham, Durham DH1 3LE, UK

Accepted 2018 May 3. Received 2018 April 24; in original form 2018 March 16

ABSTRACT

We report the discovery of a new low-redshift galaxy-scale gravitational lens, identified from a systematic search of publicly available MUSE observations. The lens galaxy, 2MASXJ04035024−0239275, is a giant elliptical at z= 0.066 04 with a velocity dispersion of $\sigma = 314\,\mathrm{km\,s^{-1}}$. The lensed source has a redshift of 0.191 65 and forms a pair of bright images on either side of the lens centre. The Einstein radius is 1.5 arcsec, projecting to 1.8 kpc, which is just one quarter of the galaxy effective radius. After correcting for an estimated 19 per cent dark matter contribution, we find that the stellar mass-to-light ratio from lensing is consistent with that expected for a Milky Way initial mass function (IMF). Combining the new system with three previously studied low-redshift lenses of similar σ, the derived mean mass excess factor (relative to a Kroupa IMF) is $\langle\alpha\rangle = 1.09 \pm 0.08$. With all four systems, the intrinsic scatter in α for massive elliptical galaxies can be limited to <0.32, at 90 per cent confidence.

Key words: gravitational lensing: strong – galaxies: elliptical and lenticular, cD – galaxies: stellar content.

1 INTRODUCTION

The initial mass function (IMF) is fundamental to understanding galaxy formation and evolution, as well as to interpreting observed properties (e.g. estimating stellar masses). Within the different star-forming environments in the Milky Way (MW), the stellar IMF is well constrained, and approximately invariant (Bastian, Covey & Meyer 2010; Offner et al. 2014). Deviations towards a flatter IMF have been reported for some resolved ultrafaint Local Group dwarfs (Geha et al. 2013).

For galaxies beyond the Local Group, resolved studies are not possible, and the IMF must be inferred from the integrated light and/or gravitational mass tracers. Broadly the observational techniques fall into two categories. The first method infers the stellar population via high signal-to-noise spectroscopy. The strength of gravity sensitive absorption lines is measured by fitting detailed stellar population synthesis templates. The second method indirectly measures the stellar population by comparing a stellar mass-to-light ratio (M/L) measured from stellar dynamics or strong lensing, to a reference M/L from a fixed IMF stellar population model. Studies independently utilizing both techniques have found evidence for an increasingly 'heavy' IMF (more measured mass than a fixed IMF model predicts) in the most massive Early Type Galaxiess (ETGs) (e.g. Treu et al. 2010; Cappellari et al. 2012; Conroy & van Dokkum 2012b; La Barbera et al. 2013).

The mass measurements from gravitational lensing require careful treatment to disentangle the contributions of stellar mass and dark matter (DM). For example, Treu et al. (2010) analysed lenses at $z \sim 0.2$ by combining lensing and stellar kinematics to constrain the parameters of a two-component mass model. This approach involves several assumptions (spherical geometry, constant stellar mass-to-light ratio, etc.). In contrast, *nearby* ($z \leq 0.1$) lenses offer a geometry in which the Einstein radius ($R_{\rm Ein}$) is reached at smaller physical radii and hence probes the dense stellar-dominated core. In such cases the relative uncertainty from DM is minimized, as the ratio of dark to stellar matter is reduced and 'pure' lensing constraints on the stellar mass can be obtained (i.e. with no additional information from stellar kinematics).

At present, the best studied $z < 0.1$ lensing ellipticals are those discovered from the SINFONI Nearby Elliptical Lens Locator Survey (SNELLS) (Smith, Lucey & Conroy 2015). This targeted approach used an integral field unit (IFU) to search for background emitters behind massive elliptical galaxies, finding SNL-1 ($z = 0.031$) and SNL-2 (z= 0.052), and 'rediscovering' the previously known lens SNL-0 ($z = 0.034$) (Smith et al. 2005; Smith & Lucey 2013). The SNELLS galaxies yielded lensing masses in strong disagreement with 'heavy' IMFs for massive ETGs, instead measuring M/L consistent with an MW-like IMF (Kroupa 2001), both in low-resolution ground-based (Smith et al. 2015), and in high-resolution space-based observations (Collier, Smith & Lucey 2018).

With only three galaxies, the possibility that the SNELLS sample *by chance* was drawn from the 'tail' of an intrinsically broad distribution in IMFs cannot be ruled out. As such, with low-number

★ E-mail: william.p.collier@durham.ac.uk

statistics, increasing the sample size is essential to investigate further this conclusion, and to test whether these lenses are representative of the parent population.

Discovering low-redshift lenses is challenging due to the high surface brightness of the massive foreground galaxy. While SNELLS pre-selected high-probability lenses using velocity dispersion measurements, an alternative approach exploiting large multi-IFU surveys like SAMI and MaNGA (Bryant et al. 2015; Bundy et al. 2015) has recently yielded new systems (Smith 2017; Talbot et al. 2018). A third technique, which we are currently pursuing, is to search for lensed line emitters behind galaxies targeted for other science goals, using data from public archives. Observations made with MUSE (Multi-Unit Spectroscopic Explorer) (Bacon et al. 2014) on the European Southern Observatory (ESO) Very Large Telescope are well suited to this method, due to the very high sensitivity and wide spectral range (4350–9300 Å) of the instrument.

In this paper, we present the discovery of the first multiply imaged strong gravitational lens from this programme. In Section 2, we briefly describe the modified lens search process. In Section 3 we present the new lens system properties. In Section 4 we present lensing mass constraints and the IMF mass excess parameter, and then compare, and combine our results with the SNELLS sample in Section 5.

2 A MUSE ARCHIVAL LENS SEARCH

Our new lensing system was identified in the course of a systematic search for multiply imaged line emitters behind low-redshift ETGs in public archival MUSE data. A full description of this programme will be presented elsewhere (Collier et al., in preparation); here, we briefly summarize the sample selection and main processing steps, to provide context for the new discovery.

For this lens search, we are analysing public MUSE observations which overlap with luminous nearby galaxies selected from the 2MASS Redshift Survey (Huchra et al. 2012). We focus our search on targets with redshift 5000 $\mathrm{km\,s^{-1}} < cz < 20\,000\ \mathrm{km\,s^{-1}}$, and $M_K < -25.7$.

The analysis begins with 'Phase 3' pipeline-reduced products retrieved from the ESO Science Archive. Our primary goal is to detect faint lensed background emitters behind the central regions of nearby ETGs. Before attempting line detection, we therefore process the pipeline-reduced data cubes to subtract the bright stellar foreground, effectively fitting elliptical isophote models to each wavelength channel. The residual cubes are noise-normalized and filtered to suppress instrumental artefacts.

Candidate emission lines are then identified above a significance threshold in the processed residual cubes. Spectra for likely sources are extracted, and redshifts are estimated automatically using MARZ (Hinton et al. 2016). Finally, the resulting object catalogue is visually inspected, and searched for any spatially separated line emitters with similar redshifts, which are potentially multiply imaged background galaxies.

Although we optimize our search method to detect faint background emission, the first galaxy-scale lens discovered was over 100 times brighter than our detection limit. Hence we report this system as a 'special case' in this paper.

3 THE NEW LENS

2MASXJ04035024−0239275 (hereafter J0403) is a luminous ($M_K = -25.7$) elliptical galaxy at heliocentric redshift $z_\mathrm{H} = 0.066\,55$ (Jones et al. 2009). In imaging from the Pan-STARRS PS1 survey (Chambers et al. 2016) J0403 shows a smooth inner light profile, well fitted by a Sérsic profile with index $n \approx 4$. In the outer regions (radius $>$ 20 arcsec), some low-surface-brightness (i band $\sim$25 mag arcsec^{-2}) tidal structures are visible. J0403 is a relatively isolated galaxy, with no overdensity of similar-colour objects visible in PS1 imaging. The closest comparable brightness companion (2MASXJ04034531−0236595) is a spiral galaxy, fainter by 1.3 mag, with relative velocity +550 $\mathrm{km\,s^{-1}}$, at a projected distance of $\sim$210 kpc (2.7 arcmin). There are no catalogued clusters with comparable redshift within a radius of 2 deg (9.5 Mpc).

J0403 was observed with MUSE as part of a study targeting supernova hosts [ESO programme 098.D-0115(A); PI L. Galbany]. The exposure time was $\sim$2400 s, with seeing $\lesssim$0.8 arcsec (estimated full width at half-maximum from compact sources). The MUSE field of view is 1 × 1 arcmin^2 ($\sim$80 × 80 kpc^2).

In the MUSE data (Fig. 1a), the light profile of J0403 is smooth at small radii, with evidence for the faint tidal features seen in the PS1 imaging. Extracting narrow-band images (Fig.1b) highlights a pair of extended background emitters (arcs A and B) either side of the galaxy centre. Strong Hα, [O III], and Hβ lines are present in the spectra of both emitters, with the same redshift, $z_\mathrm{H} = 0.191\,65$ (Fig.2). The respective velocity offset between A and B is $\leq$50 $\mathrm{km\,s^{-1}}$, providing strong evidence of a common source. When the continuum is subtracted, image A shows slight curvature at low-surface-brightness levels (Fig.1c). There is some evidence of a small velocity gradient ($\sim$50 $\mathrm{km\,s^{-1}}$ peak-to-peak) across arc A, which is mirrored in arc B. A broad-band counterpart to arc A is readily visible in the PS1 imaging, and the counter-arc is recovered after subtraction of a smooth light profile for J0403. The balance of evidence in this case strongly favours a lensing interpretation.[1]

The lensed images are separated by 2.94 ± 0.06 arcsec ($\sim$3.75 kpc), where the uncertainty is derived from measurements at various emission lines. For our lensing analysis we adopt R_Ein as half of the image separation, 1.47 ± 0.03 arcsec, and extract an aperture spectrum ($\leq R_\mathrm{Ein}$) of J0403, shown in Fig. 3. The spectrum displays the strong absorption features typical of an old stellar population, with strong Na D, Mg I, and TiO, along with weak H α and H β emission. The measured heliocentric redshift, $z_\mathrm{H} = 0.066\,04$, and velocity dispersion of $\sigma = 314 \pm 5\ \mathrm{km\,s^{-1}}$ are found by fitting this central region using PPXF (Cappellari & Emsellem 2004).

Using i-band imaging from the Pan-STARRS (PS1) survey we measure a total magnitude for J0403 of 14.26 ± 0.04 mag and an effective (half-light) radius of 5.7 arcsec (i.e. 3.9 times the size of R_Ein). Within R_Ein we measure an aperture magnitude of 16.35 ± 0.01 mag. As the PS1 point spread function (PSF; $\sim$1.1 arcsec) is comparable in size to R_Ein, a PSF correction is necessary. We determine the correction by fitting a Sérsic model via GALFIT (Peng et al. 2010), with a convolution kernel derived from a set of adjacent stars. The magnitude difference between the Sérsic model before and after convolution was 0.22 ± 0.02 mag and hence we adopt a PSF-corrected Einstein-aperture magnitude of $i_\mathrm{Ein} = 16.13 \pm 0.02$ mag.

4 LENSING MASS AND THE IMF

Gravitational lensing provides a precise measurement of the total projected mass within the Einstein radius (M_Ein). Measuring M_Ein and the luminosity within the same aperture (L_Ein), the resulting

[1] After the submission of our paper, Galbany et al. (2018), independently reported the discovery of this lens.

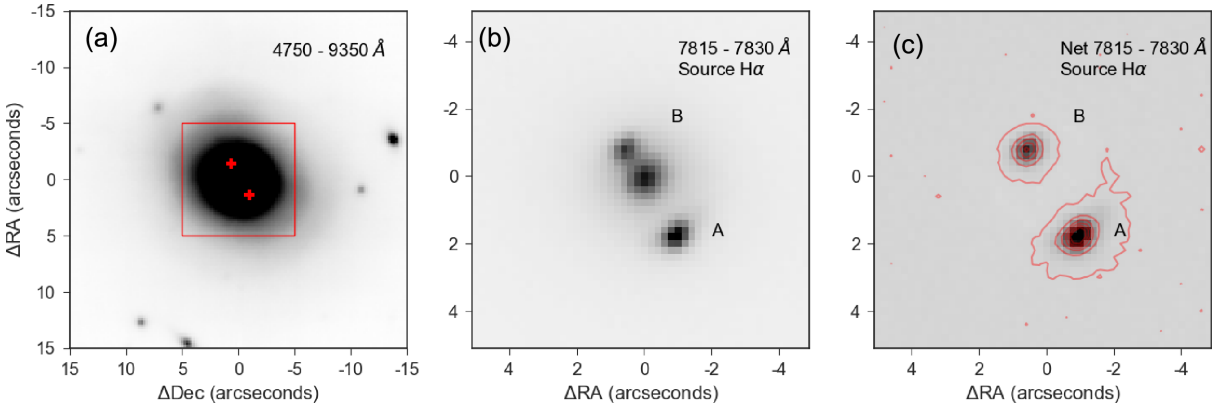

Figure 1. MUSE data of J0403, within different wavelength ranges (shown in the top right). Panel (a) displays a broad-band image collapsed over the entire MUSE wavelength range, displaying the lens structure. The red crosses mark the arc positions, while the red box encompasses the region shown in panels (b) and (c). In (b) we collapse about the H α line in the background source, revealing arcs A and B, separated by 2.94 ± 0.06 arcsec, without the need for lens subtraction. Panel (c) shows the continuum-subtracted image at the same wavelength, with contours to show the outer isophotes of the arcs.

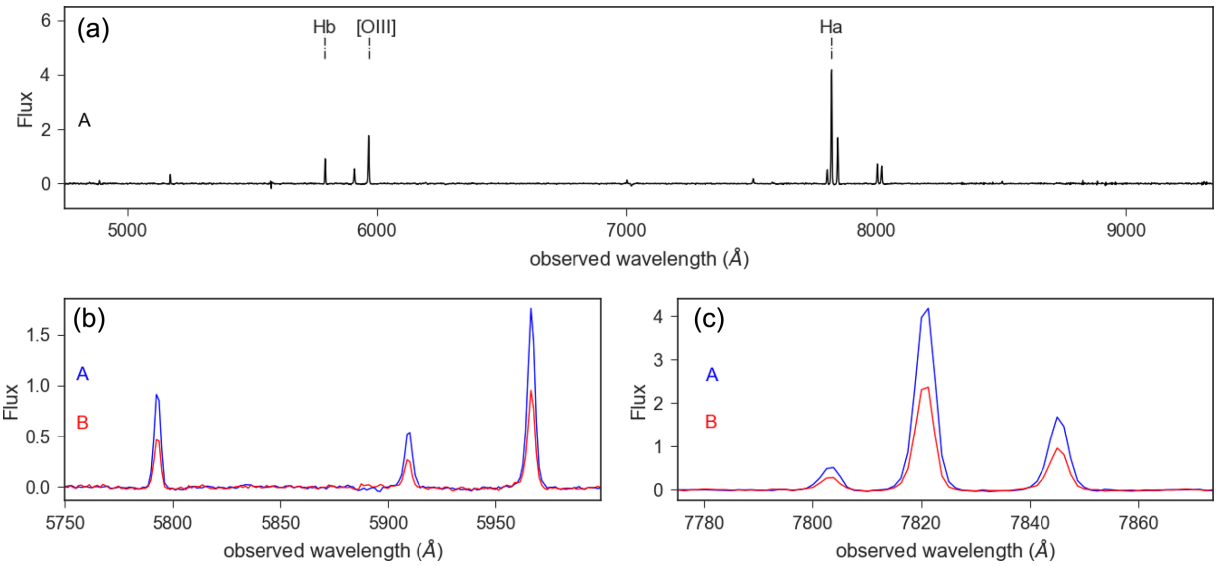

Figure 2. MUSE spectra of the lensed images, with flux in units of 10^{-16} erg s^{-1} cm^{-2} Å^{-1}. In (a) we display the arc spectrum extracted from a continuum-subtracted residual data cube, showing the bright H α, [N II], [O III], H β, H γ, and [S II] emission lines, at a redshift of 0.191 65. In (b) and (c), we overlay the emission from images A and B, for the [OIII] and H α regions, respectively. There is negligible velocity offset ($\lesssim$50 km s^{-1}) between the two spectra, and image A has been subject to a greater magnification.

mass-to-light ratio can be related to the IMF mass excess parameter, α. This factor is defined as

$$\alpha = \frac{\Upsilon}{\Upsilon_{\rm Ref}} = \frac{M^{*}_{\rm Ein}}{L_{\rm Ein}} \times \frac{1}{\Upsilon_{\rm Ref}} = \frac{M_{\rm Ein} - M^{\rm DM}_{\rm Ein}}{\Upsilon_{\rm Ref} L_{\rm Ein}} \ ,$$

where $M^{\rm DM}_{\rm Ein}$ is the dark matter component. We compare Υ, the observed stellar mass-to-light ratio, to $\Upsilon_{\rm Ref}$, a reference mass-to-light ratio for a modelled stellar population with comparable properties (i.e. metallicity, age), with a fixed Kroupa (2001) IMF. Hence a Kroupa IMF has $\alpha = 1$ by definition, while a Salpeter IMF (Salpeter 1955), with more low-mass stars, has $\alpha = 1.55$.

We compute $M_{\rm Ein}$ using the symmetric lens equation (see Smith et al. 2015, section 4.1). We adopt cosmological parameters from the 7-yr *Wilkinson Microwave Anisotropy Probe* (*WMAP*), i.e. $H_0 = 70.4$ km s^{-1} Mpc^{-1}, $\Omega_{\rm m} = 0.272$, and $\Omega_\Lambda = 0.728$ (Komatsu et al. 2011), to calculate the lensing geometry for redshifts in the CMB frame ($z_{\rm CMB} = 0.065\,69, 0.191\,30$ and $\frac{D_{\rm l} D_{\rm s}}{D_{\rm ls}} = 400.5$ Mpc).

We derive a total projected mass, $M_{\rm Ein} = 10.64 \pm 0.23 \times 10^{10}\,{\rm M}_\odot$, with the 2 per cent uncertainty dominated by the measurement of $R_{\rm Ein}$. Including a small ellipticity ($e \approx 0.1$ as measured from GALFIT) increases the mass by 3 per cent, and the inclusion of a small external shear (<5/1 per cent for SIS/SIE) reproduces the image positions perfectly. In order to account for these additional possible complexities, we revise the uncertainty in $M_{\rm Ein}$ to ∼4 per cent, i.e. $0.4 \times 10^{10}\,{\rm M}_\odot$.

The DM mass component is estimated following Smith et al. (2015), using the EAGLE hydrodynamical cosmological simulation (Schaye et al. 2015). We measure the average DM mass which would be projected inside an aperture of 1.8 kpc, averaged over all EAGLE haloes hosting galaxies with stellar velocity dispersions >275 km s^{-1}. This indicates a contribution of $M^{\rm DM}_{\rm Ein} = 2.01 \pm 0.36 \times 10^{10}\,{\rm M}_\odot$ (i.e. 19 per cent of $M_{\rm Ein}$), which yields an aperture stellar mass $M^{*}_{\rm Ein}$ of $8.63 \pm 0.54 \times 10^{10}\,{\rm M}_\odot$.

Other mass contributions within the Einstein aperture are expected to be small. For typical ETGs from the ATLAS^{3D} sample the

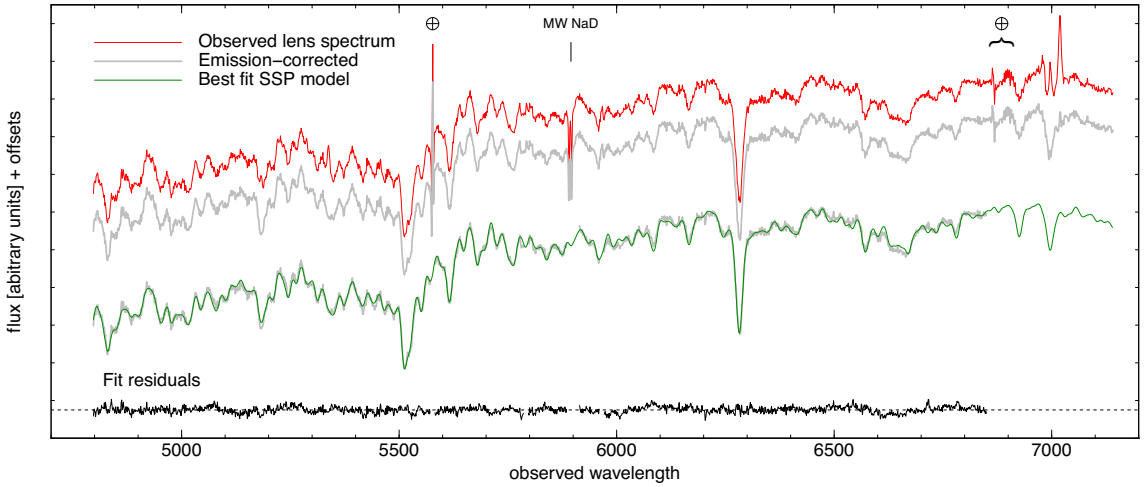

Figure 3. The MUSE spectrum of the lens galaxy J0403, extracted within the Einstein aperture, i.e. radius 1.5 arcsec, after masking pixels strongly affected by the arcs. For clarity, only the region of the MUSE spectral range (4750–6850 Å) used for fitting the stellar population models is shown. The observed spectrum (red) shows that the galaxy has an absorption-dominated spectrum, but also has a nebular line emission component, seen most easily in the H α–[N II] region. The corrected spectrum, shown in grey, after subtracting an emission-line model, fitted to the H α–[N II] complex, and assuming Case B recombination and galactic (no internal) extinction, to predict the H β emission. Below, we reproduce the emission-corrected spectrum, and show the best-fitting stellar population (green), derived from the models of Conroy & van Dokkum (2012a). This model has age 12 Gyr and metal abundances typical for massive ellipticals. The fit residuals, shown in black, have a 1 per cent rms. In fitting this model, we exclude the H α region, as well as wavelengths contaminated by atmospheric artefacts (indicated by $\oplus$) and the MW neutral sodium doublet.

gas contribution measured within $2R_{\rm eff}$ is $\sim 10^9\,{\rm M}_\odot$ for the cold gas (Young et al. 2011, 2018), and $\sim 10^9\,{\rm M}_\odot$ for the hot gas (Su et al. 2015). As the Einstein aperture is significantly smaller than this, the gas contribution is expected to be less than 1 per cent of the measured lensing mass. The average contribution from a black hole hosted by a comparable ($\sigma \approx 300$ kms^{-1}) galaxy is $\sim 2 \times 10^9\,{\rm M}_\odot$ (van den Bosch 2016), i.e. $\sim$2 per cent of the lensing mass. We do not apply a correction for these effects.

The lens aperture luminosity is calculated from the PSF corrected $i_{\rm Ein}$, with additional corrections for the line-of-sight galactic extinction and the k-correction.

Despite being located at fairly high galactic latitude ($b = -38^\circ$), J0403 lies in a region of relatively high galactic extinction, with $A_i = 0.26$ according to the Schlafly & Finkbeiner (2011). Alternatively, maps based on PS1 stellar photometry (Schlafly et al. 2014; Green et al. 2018) indicate slightly smaller values, with $A_i = 0.22$. The MUSE spectrum shows a clear galactic Na D absorption doublet ($\sim$1 Å equivalent width), which supports the presence of substantial interstellar material along this sightline. We adopt a correction of 0.24 mag, and allocate an error of 0.04 mag (16 per cent of the extinction in magnitudes, following Schlegel, Finkbeiner & Davis (1998). The k-correction is estimated from the lens g–i colour index (1.7) to be $k_i = 0.04 \pm 0.01$ mag (Chilingarian, Melchior & Zolotukhin 2010; Chilingarian & Zolotukhin 2012).

The final corrected Einstein-aperture apparent magnitude is $i_{\rm Ein} = 15.87 \pm 0.05$, which for the adopted cosmology ($D_{\rm L} = 295.7$ Mpc), and the solar AB i-band absolute magnitude of 4.534 (Blanton & Roweis 2007), yields an aperture luminosity of $2.59 \pm 0.12 \times 10^{10}\,{\rm L}_\odot$. The uncertainty is dominated by the applied corrections. Combined with $M^*_{\rm Ein}$ the observed stellar mass-to-light ratio is $\Upsilon = 3.33 \pm 0.26$ solar units.

To convert from mass-to-light ratio (Υ) to the IMF mass factor α, we need an estimate for the reference mass-to-light ratio for a given fiducial IMF (here Kroupa 2001), which depends on the stellar population properties: age (or star formation history), metallicity, etc. To estimate these parameters, we make use of the MUSE spectrum of the lens galaxy extracted within the Einstein aperture, shown in Fig.3 (red line). However, the presence of significant nebular emission, combined with limited spectral coverage in the blue, presents some challenges. Specifically, the stellar population age is constrained only by the H α and H β absorption lines, but both are contaminated by gas emission, to different extent.

We tackle the nebular emission by first fitting a three-Gaussian model to the H α and [N II] lines, with an assumed stellar continuum model. The relative amplitudes of the [N II] lines are fixed, and all lines are assumed to have the same velocity and width. The amplitudes of H α and the [N II] doublet are allowed to vary. From this model, we can predict the H β emission line, assuming Case B recombination for the intrinsic line ratio, and a relative attenuation factor of 1.135 for H β from the MW extinction (we assume no internal extinction for this exercise). Because the underlying H α absorption has only low sensitivity to the stellar population age, the emission correction is quite robust against changes to the age assumed in the first step.

After making this correction to remove the emission-infilling of the spectrum at H β, we perform a full-spectrum fit over the interval 4500–6400 Å, using single-burst models from Conroy & van Dokkum (2012b), (Fig. 3, green). We allow for variation in abundances of Mg, Fe, Na, and C, as well as variation in age. Formally, the fit implies an old population, with age 12.0 ± 1.0 Gyr, high metallicity [Z/H] $\approx$ [Mg/H] $\approx +0.15 \pm 0.02$ and typical massive elliptical galaxy abundance ratios [Mg/Fe] $\approx +0.3$, [Na/Fe] $\approx +0.5$, and [C/Fe] $\approx +0.2$.

The reference mass-to-light ratio is estimated with Conroy, Gunn & White (2009) stellar population models accessed via EZGAL (Mancone & Gonzalez 2012). For a Kroupa (2001) IMF, with an old, solar metallicity stellar population ($z_{\rm form} = 3$), the models predict $\Upsilon^*_{\rm Ref} = 2.90 \pm 0.10$. The uncertainty is derived from small vari-

ations in the metallicity and age (e.g. $z_{\rm form}$= 2.5–3.5, metallicity 1–1.5 solar). The resulting IMF mass excess parameter, with its statistical error, is $\alpha = 1.15 \pm 0.10$.

Several adopted parameters and assumptions affect the value of α derived above. If we had prescribed the Planck Collaboration XIII (2016) cosmology, α would be 4 per cent lower, due to the variation in H_0. If we had attributed the total lensing mass entirely to the stellar component (i.e. no DM inside $R_{\rm Ein}$), we would have found $\alpha = 1.42$, a 25 per cent increase. If we had assumed, due to the limited blue (most age sensitive) coverage from MUSE, that the population may be 8.5 Gyr old ($z_{\rm form} = 1.5$), α would have increased by 14 per cent. If we had adopted the Maraston (2005) models, α would increase by 10 per cent.

5 DISCUSSION AND CONCLUSIONS

We have discovered a new low-redshift gravitational lens, with a bright background galaxy, and a small Einstein radius, probing the stellar-dominated core of a massive elliptical galaxy. We have measured the lensing mass and the *i*-band Einstein aperture luminosity to estimate the IMF mismatch parameter, $\alpha = 1.15 \pm 0.10$. We attribute a further uncertainty of (∼15 per cent) ± 0.17 for the systematics. This measurement hence favours a lightweight (MW-like) IMF, rather than a heavy (e.g. Salpeter) one.

In comparison to the SNELLS systems, J0403 is more distant ($z_{\rm lens} = 0.066$ versus 0.031–0.052), but the background source is at much lower redshift ($z_{\rm src}$= 0.19 versus 0.93–2.14). As a result, the Einstein radius is smaller in angular terms (1.5 arcsec versus 2.2–2.9 arcsec). Thus despite the greater lens distance, $R_{\rm Ein}$ projects to a similar radius in physical units (1.8 kpc versus 1.5–2.2 kpc) or in galaxy-scale units ($0.25R_{\rm eff}$ versus 0.3–0.7 $R_{\rm eff}$). Like the SNELLS galaxies, J0403 has high velocity dispersion and metal abundances typical for massive elliptical galaxies. Furthermore, the lensing aperture mass is compatible with the SNELLS results, favouring an MW-like IMF, and inconsistent with very bottom-heavy IMFs.

Combining our estimate of α for J0403 with the three estimates from SNELLS (taking the values from Newman et al. 2017; Collier et al. 2018, i.e. SNL-0, SNL-1, SNL-2 = 1.05 ± 0.09, 1.17 ± 0.09, 0.96 ± 0.10), as shown in Fig. 4, we can infer limits on the *intrinsic* distribution of this quantity among $\sigma \approx 300$ km s^{-1} ETGs. We compute the joint likelihood of the four α measurements as a function of the unknown population mean $\langle\alpha\rangle$ and dispersion $\sigma_{\rm int}$, accounting for the measurement errors. Marginalizing over $\sigma_{\rm int}$, with a flat prior, we infer $\langle\alpha\rangle = 1.09 \pm 0.08$ (the error is larger than for a calculation which assumes no intrinsic dispersion). Marginalizing over the mean, we infer only an upper limit on the scatter, with $\sigma_{\rm int} < 0.32$ at 90 per cent confidence. (For comparison the same treatment applied to SNELLS alone yields an upper limit of $\sigma_{\rm int} < 0.7$, highlighting the impact of adding just one new measurement to the analysis.)

One important difference between J0403 and the SNELLS sample, which is relevant for future work, is that the J0403 arcs are both very bright and appear to be quite extended. Hence among all of the known low-redshift lenses, this system is uniquely suitable for pixelized lens inversion methods, which can yield much more powerful constraints on the mass distribution (e.g. Nightingale, Dye & Massey 2017; Oldham et al. 2017). Upcoming observations with *Hubble Space Telescope* will provide high-resolution images for use in such studies.

J0403 is by far the brightest lens system so far identified from our MUSE archival study. The results from the full sample, which is sensitive to much fainter background sources, will be the subject of a future paper (Collier et al. in preparation). We have also begun a programme to acquire targeted MUSE observations for selected high-likelihood lenses. The discovery of the J0403 system bodes well for the success of such searches. Together with efforts elsewhere (e.g. Talbot et al. 2018), we anticipate exploiting meaningful samples of lenses at $z \lesssim 0.1$ in the near future, to address the continuing puzzle of IMF variations in massive elliptical galaxies.

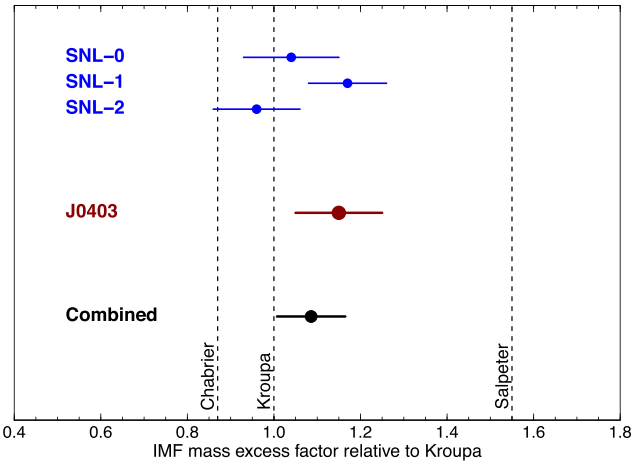

Figure 4. The distribution of the mass excess parameter (α) for the combined SNELLS and J0403 sample. In blue, is the SNELLS sample with results for SNL-0 from Newman et al. (2017), and SNL-1, SNL-2 from Collier et al. (2018). The result for J0403 from this paper is marked in red. The sample average is $\langle\alpha\rangle = 1.09 \pm 0.08$, with an inferred *intrinsic* scatter of < 0.32, at 90 per cent confidence. These galaxies on average favour an MW-like IMF in preference to a Salpeter or heavier IMF.

ACKNOWLEDGEMENTS

WPC was supported by an STFC studentship (ST/N50404X/1). RJS and JRL are supported by the STFC Durham Astronomy Consolidated Grant (ST/P000541/1). This research has made use of the NASA/IPAC Extragalactic Database (NED) which is operated by the Jet Propulsion Laboratory, California Institute of Technology, under contract with the National Aeronautics and Space Administration. This work is based on observations collected at the European Organization for Astronomical Research in the Southern hemisphere under ESO programme 098.D-0115(A), retrieved through the ESO Science Archive Facility. The Pan-STARRS1 Surveys (PS1) and the PS1 public science archive have been made possible through contributions by the Institute for Astronomy, the University of Hawaii, the Pan-STARRS Project Office, the Max-Planck Society and its participating institutes, the Max Planck Institute for Astronomy, Heidelberg and the Max Planck Institute for Extraterrestrial Physics, Garching, The Johns Hopkins University, Durham University, the University of Edinburgh, the Queen's University Belfast, the Harvard-Smithsonian Center for Astrophysics, the Las Cumbres Observatory Global Telescope Network Incorporated, the National Central University of Taiwan, the Space Telescope Science Institute, the National Aeronautics and Space Administration under Grant No. NNX08AR22G issued through the Planetary Science Division of the NASA Science Mission Directorate, the National Science Foundation Grant No. AST-1238877, the University of Maryland, Eotvos Lorand University (ELTE), the Los Alamos National Laboratory, and the Gordon and Betty Moore Foundation.

REFERENCES

Bacon R. et al., 2014, The Messenger, 157, 13
Bastian N., Covey K. R., Meyer M. R., 2010, ARA&A, 48, 339
Blanton M. R., Roweis S., 2007, AJ, 133, 734
Bryant J. J. et al., 2015, MNRAS, 447, 2857
Bundy K. et al., 2015, ApJ, 798, 7
Cappellari M., Emsellem E., 2004, PASP, 116, 138
Cappellari M. et al., 2012, Nature, 484, 485
Chambers K. C. et al., 2016, preprint (arXiv:1612.05560)
Chilingarian I. V., Zolotukhin I. Y., 2012, MNRAS, 419, 1727
Chilingarian I. V., Melchior A.-L., Zolotukhin I. Y., 2010, MNRAS, 405, 1409
Collier W. P., Smith R. J., Lucey J. R., 2018, MNRAS, 473, 1103
Conroy C., van Dokkum P., 2012a, ApJ, 747, 69
Conroy C., van Dokkum P. G., 2012b, ApJ, 760, 71
Conroy C., Gunn J. E., White M., 2009, ApJ, 699, 486
Galbany L., Collett T. E., Méndez-Abreu J., Sánchez S. F., Anderson J. P., Kuncarayakti H., 2018, preprint (arXiv:1803.09277)
Geha M. et al., 2013, ApJ, 771, 29
Green G. M. et al., 2018, preprint (arXiv:1801.03555)
Hinton S. R., Davis T. M., Lidman C., Glazebrook K., Lewis G. F., 2016, Astron. Comput., 15, 61
Huchra J. P. et al., 2012, ApJS, 199, 26
Jones D. H. et al., 2009, MNRAS, 399, 683
Komatsu E. et al., 2011, ApJS, 192, 18
Kroupa P., 2001, MNRAS, 322, 231
La Barbera F., Ferreras I., Vazdekis A., de la Rosa I. G., de Carvalho R. R., Trevisan M., Falcón-Barroso J., Ricciardelli E., 2013, MNRAS, 433, 3017
Mancone C. L., Gonzalez A. H., 2012, PASP, 124, 606
Maraston C., 2005, MNRAS, 362, 799
Newman A. B., Smith R. J., Conroy C., Villaume A., van Dokkum P., 2017, ApJ, 845, 157
Nightingale J., Dye S., Massey R., 2018, MNRAS, in press
Offner S. S. R., Clark P. C., Hennebelle P., Bastian N., Bate M. R., Hopkins P. F., Moraux E., Whitworth A. P., 2014, Protostars and Planets VI. University of Arizona Press, Chicago, IL, p. 53
Oldham L. et al., 2017, MNRAS, 465, 3185
Peng C. Y., Ho L. C., Impey C. D., Rix H.-W., 2010, AJ, 139, 2097
Planck Collaboration XIII, 2016, A&A, 594, A13
Salpeter E. E., 1955, ApJ, 121, 161
Schaye J. et al., 2015, MNRAS, 446, 521
Schlafly E. F., Finkbeiner D. P., 2011, ApJ, 737, 103
Schlafly E. F. et al., 2014, ApJ, 789, 15
Schlegel D. J., Finkbeiner D. P., Davis M., 1998, ApJ, 500, 525
Smith R. J., 2017, MNRAS, 464, L46
Smith R. J., Lucey J. R., 2013, MNRAS, 434, 1964
Smith R. J., Blakeslee J. P., Lucey J. R., Tonry J., 2005, ApJ, 625, L103
Smith R. J., Lucey J. R., Conroy C., 2015, MNRAS, 449, 3441
Su Y., Irwin J. A., White Raymond E. I., Cooper M. C., 2015, ApJ, 806, 156
Talbot M. S. et al., 2018, MNRAS, 477, 195
Treu T., Auger M. W., Koopmans L. V. E., Gavazzi R., Marshall P. J., Bolton A. S., 2010, ApJ, 709, 1195
van den Bosch R. C. E., 2016, ApJ, 831, 134
Young L. M. et al., 2011, MNRAS, 414, 940
Young L. M., Serra P., Krajnović D., Duc P.-A., 2018, MNRAS, 477, 2741

This paper has been typeset from a TEX/LATEX file prepared by the author.